Magnetic anisotropy of two trinuclear and tetranuclear $Cr^{III}Ni^{II}$ cyanide-bridged complexes with spin ground states $S = 4$ and 5†‡

Jean-Noël Rebilly,[a] Laure Catala,[a] Gaëlle Charron,[a] Guillaume Rogez,[a,b] Eric Rivière,[a] Régis Guillot,[a] Pierre Thuéry,[c] Anne-Laure Barra[d] and Talal Mallah*[a]

Received 8th December 2005, Accepted 9th February 2006
First published as an Advance Article on the web 11th May 2006
DOI: 10.1039/b517417a

The trinuclear and the tetranuclear complexes $[\{iPrtacnCr(CN)_3\}_2\{Ni(cyclam)\}](NO_3)_2\cdot 5H_2O$ **1** (cyclam = 1,4,8,11-tetraazacyclotetradecane, iPrtacn = 1,4,7-tris-isopropyl-1,4,7-triazacyclononane) and $[\{iPrtacnCr(CN)_3Ni(Me_2bpy)_2\}_2](ClO_4)_4\cdot 2CH_3CN$ **2** (Me_2bpy = 4,4′-dimethyl-2,2′-bipyridine) were synthesized by reacting $(iPrtacn)Cr(CN)_3$ with $[Ni(cyclam)](NO_3)_2$ and $[Ni(Me_2bpy)_2(H_2O)_2](ClO_4)_2$,, respectively. The crystallographic structure of the two compounds was solved. The molecular structure of complex **1** consists of a linear Cr–Ni–Cr arrangement with a central Ni(cyclam) unit surrounded by two $Cr(iPrtacn)(CN)_3$ molecules through bridging cyanides. Each peripheral chromium complex has two pending CN ligands. Complex **2** has a square planar arrangement with the metal ions occupying the vertices of the square. Each $Cr(iPrtacn)(CN)_3$ molecule has two bridging and one non-bridging cyanide ligands. The magnetic properties of the two complexes were investigated by susceptibility *vs.* temperature and magnetization *vs.* field studies. As expected from the orthogonality of the magnetic orbitals between Cr^{III} (t_{2g}^3) and Ni^{II} (e_g^2) metal ions, a ferromagnetic exchange interaction occurs leading to a spin ground states $S = 4$ and 5 for **1** and **2**, respectively. The magnetization *vs.* field studies at $T = 2$, 3 and 4 K showed the presence of a magnetic anisotropy within the ground spin states leading to zero-field splitting parameters obtained by fitting the data $D_4 = 0.36$ cm^{-1} and $D_5 = 0.19$ cm^{-1} (the indices 4 and 5 refer to the ground states of complexes **1** and **2**, respectively). In order to quantify precisely the magnitude of the axial (D) and the rhombic (E) anisotropy parameters, High-field high frequency electron paramagnetic resonance (HF-HFEPR) experiments were carried out. The best simulation of the experimental spectra (at 190 and 285 GHz) gave the following parameters for **1**: $D_4 = 0.312$ cm^{-1}, $E_4/D_4 = 0.01$, $g_{4x} = 2.003$, $g_{4y} = 2.017$ and $g_{4z} = 2.015$. For complex **2** two sets of parameters could be extracted from the EPR spectra because a doubling of the resonances were observed and assigned to the presence of complexes with slightly different structures at low temperature: $D_5 = 0.154$ (0.13) cm^{-1}, $E_5/D_5 = 0.31$ (0.31) cm^{-1}, $g_{4x} = 2.04$ (2.05), $g_{4y} = 2.05$ (2.05) and $g_{4z} = 2.03$ (2.02). The knowledge of the magnetic anisotropy parameters of the mononuclear $Cr(iPrtacn)(CN)_3$, $Ni(cyclam)(NCS)_2$ and $Ni(bpy)_2(NCS)_2$ complexes by combining HF-HFEPR studies and calculation using a software based on the angular overlap model (AOM) allowed to determine the orientation of the local ***D*** tensors of the metal ions forming the polynuclear complexes. We, subsequently, show that the anisotropy parameters of the polynuclear complexes computed from the projection of the local tensors are in excellent agreement with the experimental ones extracted from the EPR experiments.

Introduction

The discovery of the blocking of the magnetisation of the now famous $Mn_{12}ac$ complex has stimulated the research in coordination chemistry aiming to create new discrete objects (molecules) now called single molecule magnets (SMMs).[1] A single molecule magnet may be simply defined as a complex that keeps its magnetization when the magnetic field is removed after saturation has been achieved. In other words, a hysteresis loop *vs.* field is observed for such complexes due to the long relaxation time of the magnetization below a given temperature. The origin of such behaviour is the presence of a relatively high spin ground state and a non-negligible magnetic anisotropy leading to a barrier for the reversal of the magnetisation responsible of the long relaxation

[a]*ICMMO-Equipe Chimie Inorganique, CNRS UMR 8182, Université Paris-Sud, Bât 420, F-91405, Orsay, France. E-mail: mallah@icmo.u-psud.fr; Fax: (+33) 1 69154754; Tel: (+33) 1 69 15 47 49*
[b]*IPCMS-GMI, UMR CNRS 7504, 23, rue du Loess, B.P. 43, F-67034, Strasbourg Cedex 2, France*
[c]*CEA/Saclay, SCM, Bat. 125, 91191, Gif-sur-Yvette, France*
[d]*Laboratoire des Champs Magnétiques Intenses, UPR CNRS 5021, 25, avenue des Martyrs, B.P. 166, F-38042, Grenoble Cedex 9, France*

† Based on the presentation given at Dalton Discussion No. 9, 19–21st April 2006, Hulme Hall, Manchester, UK.

‡ Electronic supplementary information (ESI) available: Structural details, experimental and calculated HF-HFEPR spectra and AOM parameters for $Ni(cyclam)(NCS)_2$, $Ni(bpy)(NCS)_2$ and $Cr(iPrtacn)(CN)_3$]. See DOI: 10.1039/b517417a

time. The height of the barrier can be simply expressed for an Ising type anisotropy (easy axis of magnetization) as $|D|S^2$ (for integer spins) where D is the axial zero-field splitting parameter appearing in the spin Hamiltonian $D[S_z^2 - S(S+1)/3]$ and S the spin of the ground state. Mn_{12}ac has a ground spin state equal to 10 and a D parameter accurately determined from HF-HFEPR studies equal to -0.5 cm^{-1} (the negative sign means that the $M_S = \pm 10$ sub levels have the lowest energy or that the anisotropy is of the Ising type) which leads to a barrier of 50 cm^{-1} and a blocking of the magnetization below $T = 4$ K.[1a]

Efforts in the last ten years to prepare polynuclear complexes containing paramagnetic metal ions were rather rewarding if one considers the nuclearity of the complexes obtained.[2] Among these complexes, the highest spin ground states found were 19 ± 1, 25 and 51/2. Unfortunately, the D values associated to these states are very weak and only for two complexes the anisotropy is of the Ising type leading to a blocking of the magnetisation only below 2 K. The complexes belonging to the Mn_{12} family still hold the record for the blocking temperature. One of the objectives is to be able to prepare polynuclear complexes with a high spin ground state and a relatively large magnetic anisotropy in order to enhance the anisotropy barrier so that bistability can be present above liquid helium temperature. In order to obtain complexes with a relatively large magnetic anisotropy, one must use paramagnetic units with large anisotropy and insure the minimum of compensation between the single ion anisotropies within the cluster. Actually, in Mn_{12}ac all the 8 Mn(III) ions have their anisotropy axes (collinear to the Jahn–Teller distortion axis of Mn(III)) parallel, so that a maximum anisotropy is obtained in the ground $S = 10$ spin state. Also, it has been beautifully shown that when the Jahn–Teller axis of one or two of the eight Mn(III) is tilted, the D value of the complex decreases leading to a dramatic shift of the blocking temperature towards low temperatures.[3] Unfortunately, even though the serendipitous assembly approach lead to a large number of clusters that present the SMM behaviour, it cannot predict the arrangement of the individual metal ions within a given cluster. Even with Mn(III) ions for which anisotropy is governed by the Jahn–Teller distortion, only in very few cases the individual anisotropy axes rearrange in the right way within the clusters.

In order to be able to have a control on the magnitude of the magnetic anisotropy in polynuclear complexes, one is tempted to use a more rational approach by building the polynuclear clusters step by step. The stepwise approach allows to predict (i) the nature of the spin ground state lying on the orthogonality/overlap principles and in some cases (ii) the architecture of the final cluster. These are the necessary requirements to be able to go forward and to try to predict the anisotropy parameters of the ground state of polynuclear complexes.

One of the advantages of the rational approach is the ability for the chemist to isolate the building blocks used to prepare the clusters and to determine their magnetic anisotropy precisely. Two important questions arise: once the magnetic anisotropy of the building blocks is fully known, is it possible to compute the magnetic anisotropy of the cluster? And particularly how reliable the anisotropy parameters obtained from the calculations are when compared to the experimental values of the cluster? One of the objectives is to chemically tailor the building blocks in order to obtain high spin clusters that have large magnetic anisotropy of the Ising type, for example, if one is aiming to prepare SMMs with high blocking temperatures.

The aim of the present paper is to answer the former two questions by focusing on two simple polynuclear complexes prepared in our group namely the trinuclear $[\{iPrtacnCr(CN)_3\}_2\{Ni(cyclam)\}](NO_3)_2{\cdot}5H_2O$ **1** and the tetranuclear $[\{iPrtacnCr(CN)_3Ni(Me_2bpy)_2\}_2](ClO_4)_4{\cdot}2CH_3CN$ **2** complexes. Complex **1** is prepared from the reaction of $[Ni(cyclam)]^{2+}$ and $(iPrtacn)Cr(CN)_3$.[4] The chromium building block keeps almost the same structure within the trinuclear complex **1**. Thus, its anisotropy properties may be perfectly studied and used when calculating that of the complex **1**. The $[Ni(cyclam)]^{2+}$ is present in complex **1** but surrounded with the two nitrogen atoms from the chromium unit. In order to have a good idea of the anisotropy behaviour of the *trans*-(cyclam)Ni(NC–)$_2$ units present in complex **1**, we studied the anisotropy properties of a model complex *i.e.* *trans*-(cyclam)Ni$(NCS)_2$ and used the experimental parameters of this compound in the calculation of that of complex **1**. This method is realiable since the local structure around Ni in the model complex is mainly the same as in complex **1**. The same approach was used in the case of the tetranuclear complex **2** by using *cis*-$Ni(bpy)_2(NCS)_2$ as a model.

The anisotropy parameters D and E were determined using HF-HFEPR in most cases. In the following, the synthesis, the structure, the magnetic properties, the EPR studies and the calculation of the anisotropy parameters will be presented.

Experimental

Materials

The Ni and Cr salts were purchased from commercial sources and used as received. The $iPrtacnCr(CN)_3$ complex was prepared following the same procedure as for $(Bztacn)Cr(CN)_3$ where Bztacn is 1,4,7-tris-benzyl-1,4,7-triazacyclononane.[5]

Physical techniques

Magnetisation studies were carried out on ground crystals using a Quantum Design SQUID magnetometer in the temperature range 300–2 K within magnetic fields of 0.05 and 0.5 T. Magnetisation *vs.* field studies were performed in the field range 0–5.5 T. Diamagnetism was corrected using Pascal tables.

HF-HFEPR experiments were performed at the High Magnetic Field Laboratory, Grenoble, France, using a previously described apparatus.[6] We used ground crystals (about 100 mg) pressed to form a pellet in order to reduce torquing effect under high magnetic fields. Simulation programme is available from Dr H. Weihe; for more information see the www page: http://sophus.kiku.dk/software/epr/epr.html.[7]

Crystallographic data for complexes **1** and **2** are reported in Table 1.

CCDC reference numbers 292375 and 292376.

For crystallographic data in CIF or other electronic format see DOI: 10.1039/b517417a

Preparations

$[\{iPrtacnCr(CN)_3\}_2\{Ni(cyclam)\}](NO_3)_2{\cdot}5H_2O$ 1. 100 mg (3.4×10^{-4} mol) of $Ni(NO_3)_2{\cdot}6H_2O$ were dissolved in 20 ml of

Table 1 Crystallographic data for **1** and **2**

	1	**2**
Empirical formula	$C_{46}H_{100}N_{18}O_{11}NiCr_2$	$C_{44}H_{60}N_{11}O_8Cl_2CrNi$
M_r	1244.15	1052.65
Space group	$C2/c$	$P\bar{1}$
a/Å	17.623(4)	12.471(3)
b/Å	9.6890(19)	14.195(3)
c/Å	37.496(8)	15.050(3)
α/°		109.18(3)
β/°	100.46(3)	94.03(3)
γ/°		91.87(3)
V/Å^3	6296(2)	2505.9(9)
Z	4	2
D_c/g cm^{-3}	1.313	1.395
$F(000)$	2664	1102
T/K	123(2)	160(1)
μ(Mo-Kα)/cm^{-1}	0.701	0.760
R_1[a]	0.0935	0.0529
wR_2[b]	0.2859	0.1287
S[c]	1.036	1.021

[a] $R_1 = \sum(|F_o| - |F_c|)/\sum|F_o|$. [b] $wR_2 = \{\sum[w(F_o^2 - F_c^2)^2]/\sum[w(F_o^2)^2]\}^{1/2}$ and $w = 1/[\sigma^2(F_o^2) + (aP)^2 + bP]$ with $P = [F_o^2 + 2F_c^2]/3$, $a = 0.1716$ (**1**) and 0.0675 (**2**), and $b = 21.4203$ (**1**) and 6.7927 (**2**). [c] Goodness of fit $= [\sum w(|F_o| - |F_c|)^2/(N_o - N_p)]^{1/2}$.

methanol and added to 69 mg (3.4×10^{-4} mol) of cyclam dissolved in 10 ml of methanol. To the resulting yellow solution, 88.5 mg (2.3×10^{-4} mol) of (iPrtacn)Cr(CN)$_3$ was added as a solid and the mixture stirred until the complete dissolution of the solid. The solution was then reduced to a volume of 5 ml, 0.5 ml of ethyl acetate were added and the mixture left to stand unperturbed for three days. yellow needles were then collected (yield = 80%). The crystals were used for X-ray diffraction. Elemental analysis (%). Found: C 44.08, H, 7.95 N 20.31, Cr, 8.11 Ni 4.95. Calc. for $C_{46}H_{100}N_{18}O_{11}Cr_2Ni$: C 44.41, H 8.1, N 20.26, Cr 8.36, Ni 4.72.

[{iPrtacnCr(CN)$_3$Ni(Me$_2$bpy)$_2$}$_2$](ClO$_4$)$_4$·2CH$_3$CN 2. To 50 mg (1.3×10^{-4} mol) of Ni(ClO$_4$)$_2$·6H$_2$O dissolved in 20 ml of acetonitrile were added 51 mg (2.6×10^{-4} mol) of Me$_2$bpy (4,4′-dimethyl-2,2′-bipyridine). The mixture was stirred until complete dissolution of the bipyridine and then 53 mg (1.3×10^{-4} mol) of iPrtacnCr(CN)$_3$ were added as a solid leading almost immediately to an orange solution. Cubic orange crystals were obtained after several days by the diffusion of *tert*-butyl methyl ether into the mother solution, Yield = 80%. Elemental analysis (%). Found: C 47.74, H, 5.91 N 13.26, Cl 7.01 Cr, 4.92 Ni 5.55. Calc. for $C_{47}H_{102}N_{18}O_{13}Cr_2Ni$: C 47.83, H 5.61, N 13.38, Cl 6.95, Cr 4.98, Ni 5.55.

Results and discussion

Description of the structures

[{iPrtacnCr(CN)$_3$}$_2${Ni(cyclam)}](NO$_3$)$_2$·5H$_2$O, 1. The structure of **1** is comprised of the trinuclear dication [{iPrtacnCr(CN)$_3$}$_2${Ni(cyclam)}$^{2+}$, nitrates as anions and solvent molecules. The Ni atom lies on an inversion centre and the cyclam moiety is rotationally disordered over two positions. As expected from the presence of two available sites on the Ni(cyclam) unit, two chromium complexes are linked to the nickel atom in *trans* position by bridging cyanides (Fig. 1, Table 1). The geometry around Ni is a slightly distorted octahedron with Ni–N_{NC} bond lengths of 2.128 Å and slightly shorter Ni–N_{cyclam} (2.03 and 2.12 Å). It is very close to that of *trans*-Ni(cyclam)(NCS)$_2$ where the longest Ni–N bond lengths are with the NCS nitrogen atoms (see ESI,‡ Fig. S1, Table S1).[8] The geometry around Cr is close to a distorted octahedron along one of its three-fold symmetry axis, the Cr–C_{CN} bond lengths are almost equal (2.069(8), 2.075(8) and 2.075(7) Å). The bite angles of the iPrtacn ligand range from 84.4 to 85.3° and the C_{CN}–Cr–C_{CN} angles are almost equal (83.5, 83.7 and 83.7°). Selected bond lengths and angles are given in Table 2. It is thus reasonable, if one consider the first coordination sphere around Cr, to assume that the complex has a three-fold symmetry axis. The structure of the mononuclear (iPrtacn)Cr(CN)$_3$ complex was solved and the geometry around Cr is almost the same as in complex **1** (see ESI,‡ Fig. S2, Table S2). The Ni–N_{CN}–C angle is equal to 156.2°, much smaller than what was found (170°) for a similar complex reported by Long and co-workers.[4]

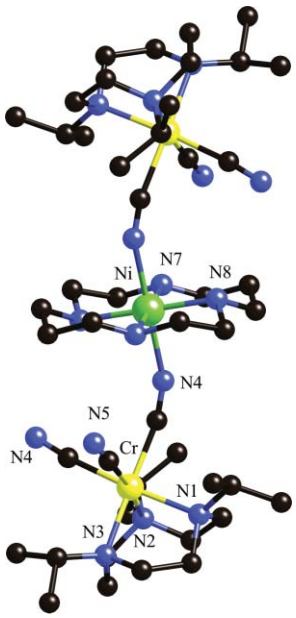

Fig. 1 View of the molecular structure of the trinuclear complex [{iPrtacnCr(CN)$_3$}$_2${Ni(cyclam)}]$^{2+}$.

[{iPrtacnCr(CN)$_3$Ni(Me$_2$bpy)$_2$}$_2$](ClO$_4$)$_4$·2CH$_3$CN 2. The structure of **2** is comprised of a square-like tetranuclear Cr_2Ni_2 cation, four perchlorates and solvent molecules. The metal ions occupy the vertices of the square which consists of two dimeric Cr–Ni units linked together by a inversion centre. (Fig. 2). Each chromium unit has one non-bridging and two bridging cyanides. The geometry around the chromium is mainly the same as in complex **1**. The

Table 2 Selected bond lengths (Å) and angles (°) for **1**

Ni–N10	2.061(12)	Cr–C18	2.069(8)
Ni–N8	2.03(2)	Cr–C16	2.075(8)
Ni–N9	2.059(12)	Cr–C17	2.075(7)
Ni–N7	2.12(2)	Cr–N3	2.130(6)
Ni–N4	2.128(6)	Cr–N2	2.144(6)
Cr–N1	2.159(6)		
N4–C16	1.139(9)		
(Cr–(CN)–Ni)			
C16–N4–Ni	156.2(6)	N4–C16–Cr	165.2(6)

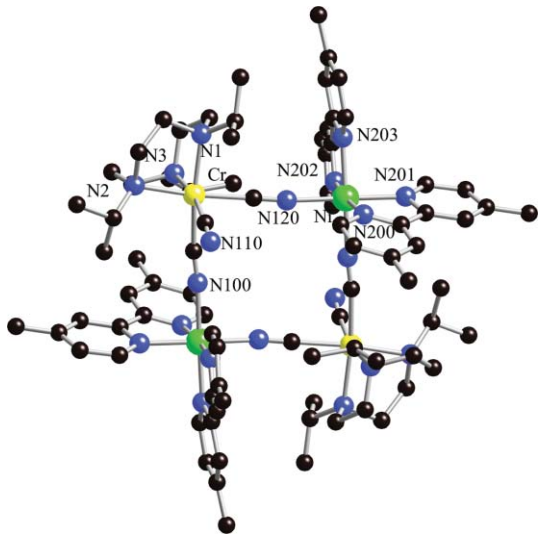

Fig. 2 View of the molecular structure of the tetranuclear complex $[\{iPrtacnCr(CN)_3Ni(Me_2bpy)_2\}_2]^{4+}$.

Ni–N bond lengths are almost identical ranging from 2.09 to 2.07 Å. The $N_{CN}NiN_{CN}$ angle is equal to 90.4° and the bite angles of the Me_2bpy are around 78°. When the local geometry around Ni is compared to that of $Ni(bpy)_2(NCS)_2$, the main differences are found for the two *trans* Ni–N_{bpy} bond lengths which are longer in the latter (2.10 instead of 2.08 Å). And one Ni–N_{NCS} is found shorter that the analogue Ni–N_{NC} in complex **2** (2.03 instead of 2.08 Å) (see ESI,‡ Fig. S3, Table S3). The angles for the two structures are almost identical. The Cr–CN–Ni linkage is almost linear with Cr–C_{CN}–N and Ni–N_{CN}–C angles larger than 169°. The Ni–N distances are those expected and range from 2.07 to 2.10 Å (Table 3).

Table 3 Selected bond lengths (Å) and angles (°) for **2**

Ni1–N120	2.071(4)	Cr1–C120	2.067(5)
Ni1–N100	2.081(4)	Cr1–C100^a	2.068(4)
Ni1–N202	2.081(4)	Cr1–C110	2.115(5)
Ni1–N201	2.088(4)	Cr1–N2	2.163(4)
Ni1–N200	2.093(4)	Cr1–N1	2.165(4)
Ni1–N203	2.098(4)	Cr1–N3	2.182(4
C110–N110	1.047(6)	N120–C120	1.147(5)
C100–N100	1.151(5)	N100–C100–Cr1^a	170.5(4)
N120–Ni1–N100	92.05(14)	N202–Ni1–N200	173.02(15)
N120–Ni1–N202	90.72(15)	N201–Ni1–N200	79.08(15)
N100–Ni1–N202	94.29(14)	N120–Ni1–N203	88.43(14)
N120–Ni1–N201	175.28(15)	N100–Ni1–N203	172.35(14)
N100–Ni1–N201	88.31(14)	N202–Ni1–N203	78.07(14)
N202–Ni1–N201	93.95(15)	N201–Ni1–N203	91.84(14)
N120–Ni1–N200	96.26(15)	N200–Ni1–N203	102.09(14
N100–Ni1–N200	85.45(14)	C120–Cr1–C100^a	84.98(16)
C120–Cr1–C110	84.33(16)	C100–Cr1–C110^a	82.64(16)
C120–Cr1–N2	169.40(15)	C100^a–Cr1–N2	103.27(15)
C110–Cr1–N2	90.07(15)	C120–Cr1–N1	88.03(15)
C100^a–Cr1–N1	170.35(16)	C110–Cr1–N1	103.30(15)
N2–Cr1–N1	84.50(14)	C120–Cr1–N3	102.93(16)
C100^a–Cr1–N3	90.12(15)	C110–Cr1–N3	169.31(15)
N2–Cr1–N3	83.93(14)	N1–Cr1–N3	84.97(14)
C200–N200–Ni1	126.6(3)	C120–N120–Ni1	169.2(4)
C100–N100–Ni1	174.7(4)	N110–C110–Cr1	169.2(4)

^{a} $1-x, 1-y, 2-z$.

The analysis of the three-dimensional structure shows the presence of two-dimensional interactions along the *c* and the *a** crystallographic axes. Along the *c* direction (Fig 3), the interaction is mainly due to short C–C (3.44 Å) distances between a carbon atom belonging to the methyl group of a Me_2bpy ligand and that of a carbon atom from the pyridine group of the symmetry equivalent ligand. The interactions along the *a** direction involve the carbon atoms (3.47 Å) of the pyridine linked to the methyl groups (Fig. 4).

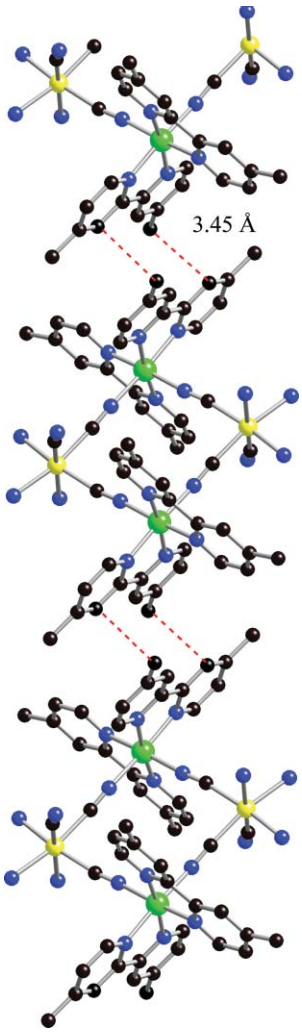

Fig. 3 Packing along the *c* direction of the crystal for **2**.

Magnetic properties

The thermal dependence of $\chi_M T$ for **1** shows an increase of $\chi_M T$ upon cooling from room temperature with a maximum value (9.17 cm^3 K mol^{-1}) at $T = 4$ K (Fig. 5). The $\chi_M T$ value at room temperature (5.17 cm^3 K mol^{-1}) is slightly larger from the expected one for isolated one Ni(II) and two Cr(III) metal ions (4.96 cm^3 K mol^{-1} assuming $g_{Cr} = 2.0$ and $g_{Ni} = 2.2$). The slight decrease of $\chi_M T$ below 4 K can, as usual, be assigned to the presence of very weak intermolecular antiferromagnetic interactions and/or zero-field splitting (magnetic anisotropy) within the ground state. The thermal dependence of $\chi_M T$ is in line with the presence of a ferromagnetic exchange interaction leading to a $S = 4$ ground

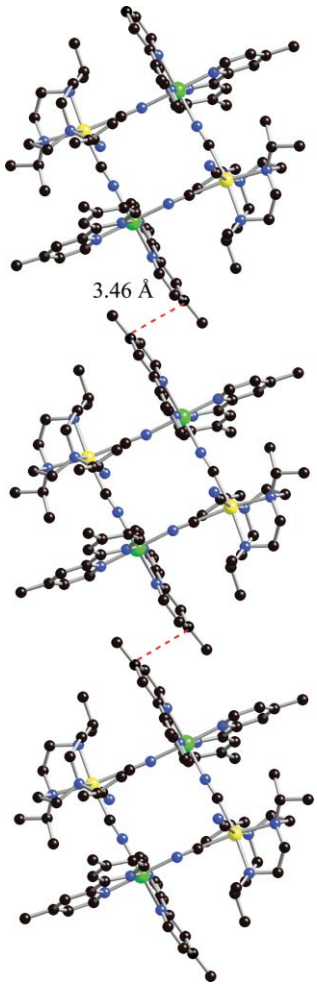

Fig. 4 Packing along the *a** direction of the crystal for **2**.

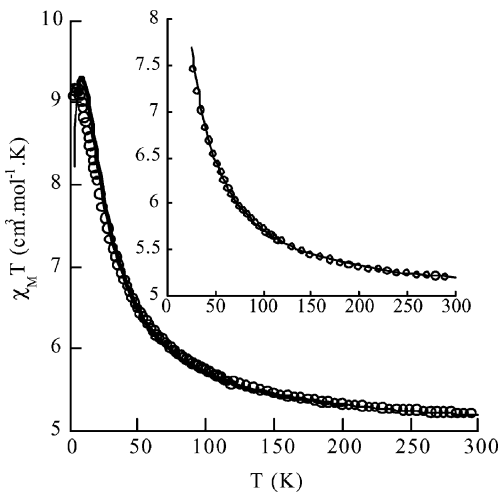

Fig. 5 $\chi_M T = f(T)$ for **1** (○) experimental and (—) best fit (see text).

state as expected from the quasi orthogonality of the magnetic orbitals.[9] The maximum value of $\chi_M T$ (9.17 cm^3 K mol^{-1}) is lower than the expected one for an isolated and isotropic $S = 4$ state (10.5 cm^3 K mol^{-1} assuming an average g-value equal to 2.05). Actually, strict orthogonality occurs when the Cr–CN–Ni linkage is linear. In complex **1**, the Ni–N–C angles (where N–C are the bridging cyanides) are quite far from linearity (155.81°) so that non-zero overlap occurs between the d_{z^2} Ni(II) and the d_{xz} (and d_{xz}) Cr(III) orbitals. Cano and Julve recently showed using DFT calculations that the antiferromagnetic contribution (due to overlap) dominates the ferromagnetic one when the Ni–N–C angle is lower than 148°.[10] Thus, for complex **1** (Ni–N–C 155.8°), one expects a relatively weak ferromagnetic interaction. The fit of the $\chi_M T = f(T)$ data were carried out considering the spin Hamiltonian $H = -J_{CrNi} S_{Ni} \cdot (S_{Cr1} + S_{Cr2})$. The first step consisted of fitting the data above $T = 30$ K in order to discard the low temperature effects (zero-field splitting and/or intermolecular interactions). An excellent fit ($R = 1 \times 10^{-5}$) is obtained for $J_{CrNi} = +10$ cm^{-1} and $g = 2.04$ (Fig. 5, inset). The next step was to fit the whole data, including the effect of the intermolecular interactions (zJ) within the mean field approximation,[11] by imposing the J and g values found. In this case, the fit leads to $zJ = -0.08$ cm^{-1} and $J_{CrNi} = 8$ cm^{-1} (Fig. 5). We did not include the effect of the anisotropy of the ground state in the fit procedure since it has the same effect as the antiferromagnetic intermolecular interactions of decreasing $\chi_M T$ at low temperature. The exchange coupling parameter value predicted by Julve and Cano from DFT calculations (12 cm^{-1}) for the same Ni–N_{CN}–C angle is in good agreement with the experimental value (10 cm^{-1}) of complex **1**. On the other hand, the similar complex reported by Long and coworkers has a J_{CrNi} value equal to 21.8 cm^{-1}. This larger value is mainly due to the Ni–N_{CN}–C angle (170°) much closer to 180° than in complex **1**. In order to confirm the nature of the spin ground state ($S = 4$) and to check the presence of magnetic anisotropy, magnetisation *vs.* field measurements were carried out at $T = 2$ and 6 K (Fig. 6). At $T = 2$ K, the magnetisation nearly reaches saturation at $\mu_0 H = 5.5$ T with a value of 7.8 μ_B slightly lower than the expected one for an isotropic $S = 4$ ground state (8.2 μ_B assuming $g = 2.05$). On the other hand, the $M = f(\mu_0 H/T)$ plots are not superimposable which is the sign of the presence of magnetic anisotropy within the ground state. Since the first excited state $S = 3$ is at 8 cm^{-1} (J_{CrNi}) above the ground state, one can reasonably assume that at temperatures below 6 K (4.2 cm^{-1}) and a magnetic field higher than 2 T, only the $S = 4$ ground state is populated. The magnetization data were fitted

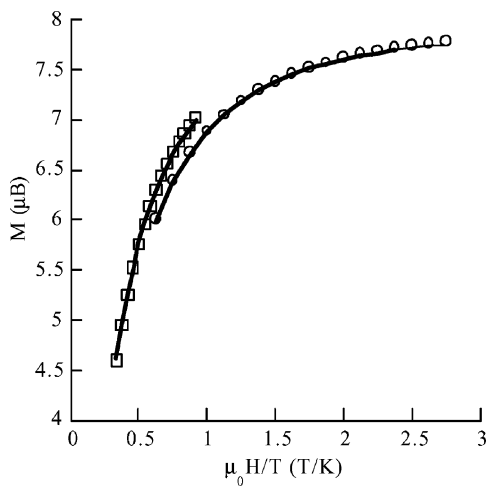

Fig. 6 $M = f(\mu_0 H/T)$ for **1** at $T = 6$ K (□, experimental) and 2 K (○, experimental), (—) best fit.

by full diagonalization of the energy matrices based on the ZFS Hamiltonian $H_{ZFS} = D_4[S_z^2 - S(S+1)/3] + E_4(S_x^2 - S_y^2)$ where D_4 and E_4 are the axial and the rhombic ZFS parameters for the ground $S = 4$ spin state, respectively, S the total spin and S_x, S_y and S_z the components of the total spin operator. The diagonalisation was carried out for 120 orientations of the magnetic field in order to reproduce the magnetization of a powder. The best fit leads to: $D_4 = 0.36$ cm^{-1}, $E/D = 0.16$ and $g = 2.0$. It is worth noting here that the magnetization studies on powder do not give precise values of the anisotropy parameters; generally only the value of the axial parameter (D) is reliable since one can obtain good fits for almost any value of the rhombic parameter without changing the value of D. As we will see in the next section, HF-HFEPR will enable a precise determination of the anisotropy parameter D_4 and E_4.

Complex **2** has a similar behaviour for the thermal variation of $\chi_M T$ *vs.* temperature (Fig. 7). At room temperature, the experimental value (7.3 cm^3 K mol^{-1}) is larger than the expected one for non-interacting 2 Ni(II) and 2 Cr(III) ions (6.17 cm^3 K mol^{-1}) assuming the same g values as above. Upon cooling, $\chi_M T$ increases and reaches a value of 26.7 cm^3 K mol^{-1} at $T =$ 5.9 K and then slightly decreases. Since the general behaviour indicates a ferromagnetic interaction between the metal ions, a spin ground state $S = 5$ and thus a $\chi_M T$ value of 15.5 cm^3 K mol^{-1} (average g value equal to 2.1) is expected at low temperature. The experimental much larger value (26.7 cm^3 K mol^{-1}) can be due to the presence of ferromagnetic intermolecular interactions within the compound. This is a reasonable assumption because of the presence of 2D interactions between the tetranuclear clusters (Fig. 3 and 4). The magnetic data were thus fitted for temperatures above 30 K in order to minimize the dependence between the intermolecular interaction parameter zJ' and the intramolecular one J'_{CrNi}. The best fit leads to $J'_{CrNi} = 26$ cm^{-1}, $zJ' = 0.05$ cm^{-1} and $g = 2.03$. The Cr–Ni exchange coupling interaction is larger than that reported by Long (21.8 cm^{-1}) even though the two compounds have the same Ni–N–C angles. The origin of this difference is probably the shorter Ni–N_{CN} distance (2.072 instead of 2.108 Å) in **2**. In order to confirm that the ground state of the tetranuclear complex **2** is indeed $S = 5$, magnetization *vs.* field studies were carried out at $T = 2$, 3, 4 and 6 K. The magnetization value obtained at $T = 2$ K and $\mu_0 H = 5.5$ T is equal to 10.4 μ_B. This corresponds well to the value expected for a ground spin state $S = 5$. The $M = f(\mu_0 H/T)$ plots (Fig. 8) at fields higher than 1 T, where the intermolecular interactions are overcome, are not superimposable indicating the presence of magnetic anisotropy within the ground $S = 5$ state. The data were fitted in the same way as for complex **1** leading to the following values: $D_5 = 0.19$ cm^{-1}, $E_5/D_5 = 0.25$, $g = 2.23$. These results show that there is an appreciable magnetic anisotropy within the ground spin state that can be determined by EPR studies.

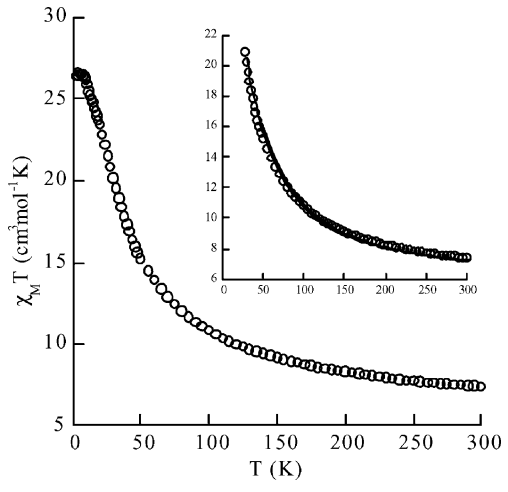

Fig. 7 $\chi_M T = f(T)$ for **2** (○) experimental and (—) best fit in the temperature region 300–30 K.

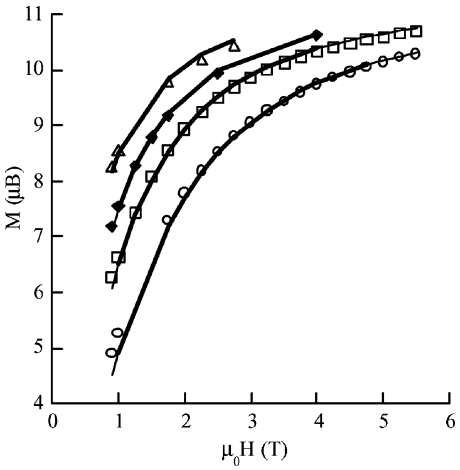

Fig. 8 $M = f(\mu_0 H/T)$ for 2 at $T = 2$ (○), 3 (□), 4 (◆) and 6 K (△), (—) best fit.

HF-HFEPR studies

The spectra of complex **1** were recorded at two different frequencies 190 GHz (6.34 cm^{-1}) at 15 K and 285 GHz (9.51 cm^{-1}) at 5 and 15 K. Since the D value for complex **1** is around 0.3 cm^{-1}, the EPR spectra at frequencies higher than 6 cm^{-1} will lead to resonances at magnetic fields higher than 4 T. This means that the Zeeman effect on the ground spin state will be dominant and the energy levels can be labelled as pure M_S sub levels. Before analysing the experimental spectra, it is interesting to plot the energy levels as a function of the magnetic field in the x, y and z directions for anisotropy parameters ($D = 0.3$ cm^{-1}, $E/D = 0.1$ and $g_{iso} = 2.1$) close to those obtained from the magnetization data (Fig. 9(a)–(c)). The energy plot diagrams with the magnetic field taken along the z direction will span the largest region of the spectra. For the present case where D_4 was taken to be positive, the transition between the ground $M_S = -4$ to -3 sublevels will be at the highest magnetic field (the reverse situation will occur for a negative D value). Thus, the resonances that appear at the highest fields will have the strongest intensities while those that should appear at the lowest fields will have the weakest intensities and may not be seen experimentally. On the other hand, since the Zeeman effect is dominant over D, the energy separation between the z resonances will be equal to $2D_4/g_z\beta\mu_0 H$. The experimental spectra at 190 GHz ($T = 15$ K) presents the features expected for the case discussed above (Fig. 10). The difference between the resonances appearing at the highest fields is around 0.63 T which leads to a value of 0.31 cm^{-1} (assuming a g_z value of 2.1) for D_4. One can then

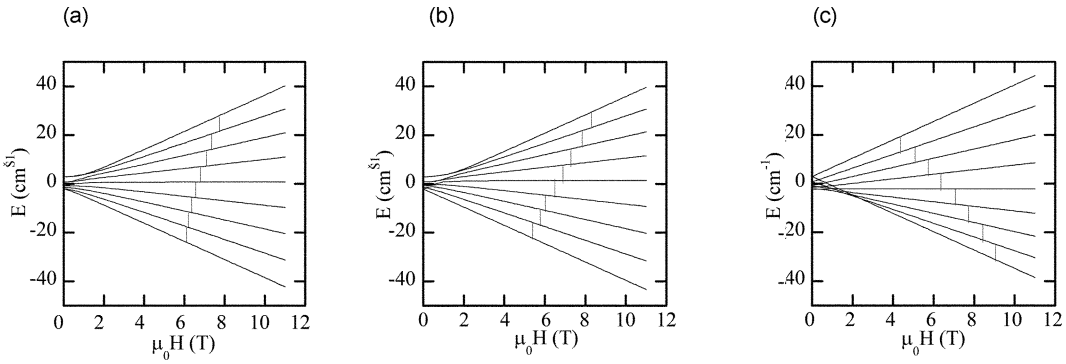

Fig. 9 (a) $E = f(\mu_0 H)$ for a spin state $S = 4$ along the x direction for $D = 0.3\ cm^{-1}$, $E/D = 0.1$ and $g_x = 2.1$. (b) $E = f(\mu_0 H)$ for a spin state $S = 4$ along the y direction for $D = 0.3\ cm^{-1}$, $E/D = 0.1$ and $g_y = 2.1$. (c) $E = f(\mu_0 H)$ for a spin state $S = 4$ along the z direction for $D = 0.3\ cm^{-1}$, $E/D = 0.1$ and $g_z = 2.1$; the incident quantum is equal to $6.34\ cm^{-1}$.

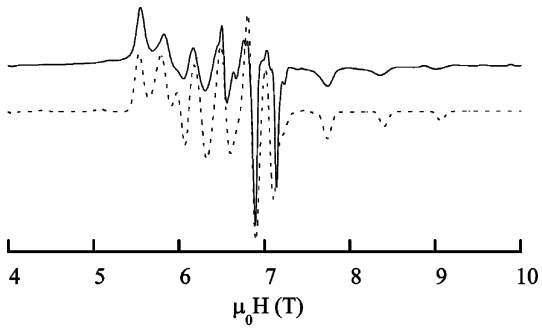

Fig. 10 EPR spectrum of complex **1** at 190 GHz and $T = 15$ K (—) experimental, (---) best simulation.

calculate that the lowest magnetic field where the resonance along the z direction should appear is around 4.2 T. No transitions are observed in the experimental spectrum below $\mu_0 H = 5.5$ T which means that at $T = 15$ K, the intensities of these resonances are too weak to be observed and thus the sign of D is positive. In the case where the rhombic parameter E_4 is equal to zero, the resonances in the x and y directions will be at the same magnetic field. The experimental spectra show many transitions between 5.5 and 7 T and a reasonable assumption is that E_4 is different from zero. On these basis, the best simulation (Fig. 10) corresponds to the following parameters: $D_4 = 0.312\ cm^{-1}$, $E_4/D_4 = 0.01$, $g_x = 2.003$, $g_y = 2.017$ and $g_z = 2.015$. The reliability of these parameters can be checked by simulating the spectrum of the complex with the same parameters as above at another frequency. Fig. 11 shows that the calculated spectrum at 285 GHz ($9.51\ cm^{-1}$) fits reasonably well the experimental one. Since the largest magnetic field available experimentally is 12 T, the resonance at the highest field expected around 12.3 T in the spectrum at 285 GHz cannot be seen. The spectra were calculated considering only the ground $S = 4$ spin state and neglecting the participation of the first excited $S = 3$ state assumed not to be enough populated at the fields were the corresponding transitions are expected.

The magnitude and the sign of the D_4 parameter obtained from EPR is very close to that extracted from the fit of the magnetisation. This confirms that the magnetization studies can give a reasonable idea on the nature of the axial magnetic anisotropy. While for the rhombic parameter E_4, the magnetisation is obviously not reliable. The degree of axiality is measured by the E_4/D_4 value (maximum rhombicity corresponds to a E/D value of 0.33). For complex **1**, this value was found equal to 0.01 which means that the $S = 4$ ground state has an almost pure axial anisotropy with an easy plane of magnetization since D is positive.

The spectra of complex **2** recorded at the same two frequencies and at $T = 15$ K have the same shape as that of complex **1** (Fig. 12 and 13). However, a close look at the high field transitions show a doubling of the resonances. Since the $S = 4$ first excited state is well above the ground $S = 5$ state ($50\ cm^{-1}$) one can reasonably exclude its participation at $T = 15$ K. A possible origin of this doubling is the presence at low temperature of a very small structural difference between two molecules that induces a slight difference in the anisotropy parameters that can be detected by EPR. We have assumed this hypothesis and making the same analysis for the

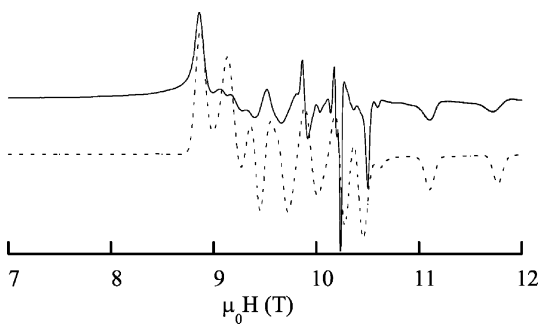

Fig. 11 EPR spectrum of complex **1** at 285 GHz and $T = 15$ K (—) experimental, (---) best simulation.

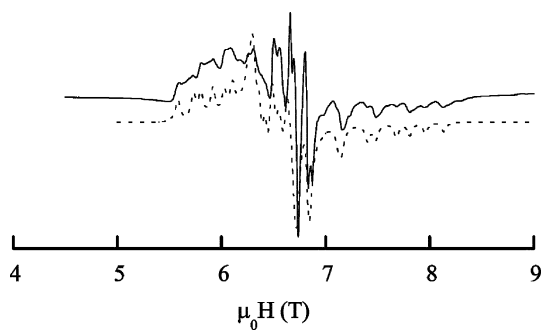

Fig. 12 EPR spectrum of complex **2** at 190 GHz and $T = 15$ K (—) experimental, (---) best simulation.

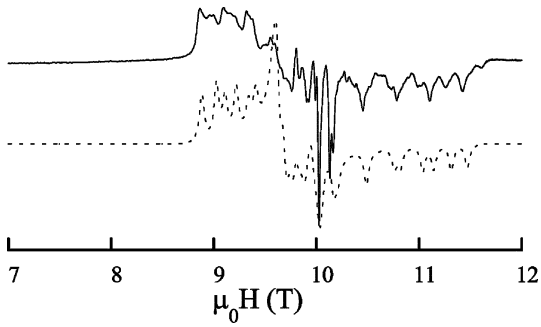

Fig. 13 EPR spectrum of complex **2** at 285 GHz and $T = 15$ K (—) experimental, (---) best simulation.

spectra as for complex **1**, it was possible to calculate two different spectra with the following parameters: $D_5 = 0.154$ cm^{-1}, $E_5 = 0.048$ cm^{-1}, $g_x = 2.04$, $g_y = 2.05$, $g_z = 2.03$ and $D'_5 = 0.13$ cm^{-1}, $E_5 = 0.04$ cm^{-1}, $g_x = 2.05$, $g_y = 2.05$, $g_z = 2.02$. The calculated spectrum for each frequency corresponds to the sum of the spectra calculated for the two sets of values.

In the case of complex **2**, the rhombicity ($E/D = 0.31$) is almost maximal while complex **1** has an axial magnetic anisotropy. In the next section we will see, knowing the anisotropy of the mononuclear complexes it is possible to estimate the expected anisotropy of the clusters and show that the calculated parameters correspond well to those extracted from EPR.

Computation of the anisotropy parameters for complexes 1 and 2

In order to estimate the values of the magnetic anisotropy parameters D and E of polynuclear complexes, one must be able to determine as accurately as possible the single ion anisotropy of the metal ions belonging to the clusters. The stepwise approach offers a unique opportunity to do so since in most cases the environment of the metal ions within the clusters are very close to that of the mononuclear complexes used to build up the final cluster. Thus, the first step is to prepare such mononuclear complexes and to study their magnetic anisotropy using resonance techniques such as EPR. In order to estimate the anisotropy parameters of a polynuclear complex from the single ion anisotropy contributions, it is necessary to determine the orientation of the single ion anisotropy tensors within the cluster. This can be achieved by calculating the D and E parameters of the mononuclear model complexes using a software based on the angular overlap model (AOM) as we have already reported on the mononuclear $[Ni(Himpy)_2(NO_3)]NO_3$ complex.[12] An output of the software gives the orientation of the anisotropy tensor with regards to the M-ligand bonds. The tensor orientation is considered to be valid if the E and D parameters extracted from the calculations succeed to well reproduce the experimental values obtained from EPR. Once the local tensors orientations of all the single ions within the cluster are known, it becomes possible to calculate the matrix elements of the total tensor corresponding to the ground spin state of the cluster using the tensorial relationship:

$$\boldsymbol{D}_S = \sum_i d_i^S \boldsymbol{D}_i + \sum_{i<j} d_{ij}^S \boldsymbol{D}_{ij} \quad (1)$$

where $\boldsymbol{D}_i$ are the local tensors, $\boldsymbol{D}_{ij}$ the tensors due to the spin–spin interactions and the coefficients d_i^S arise from the angular momentum coupling between the local spin that correspond to the total spin S considered (in the present case the ground state of the clusters).

Let us first focus on the trinuclear complex since it can be considered as a simple case where the approach presented above can be easily applied. The mononuclear units of the trinuclear complex **1** can be modelled by the (iPrtacn)Cr(CN)$_3$ and the *trans*-Ni(cyclam)(NCS)$_2$ mononuclear complexes. This can be considered as a good approximation since the local structure around Cr and Ni within complex **1** is almost the same as that of the model complexes. Furthermore, we assume the NCS ligand can model fairly well the electronic effect of the NCCr unit. In order to determine the anisotropy parameters of *trans*-Ni(cyclam)(NCS)$_2$, an analysis of its structure was performed and a HF-HFEPR study were carried out. The structure of this complex shows the presence of four crystallographically different Ni atoms with very slight structural differences. The EPR studies were carried out at 285 and 380 GHz ($T = 5$ K). The experimental spectra can be simulated by considering two sets of parameters: $D = 5.8$ cm^{-1}, $E/D = 0.07$, $g_x = 2.11$, $g_y = 2.04$, $g_z = 2.09$ and $D = 5.05$ cm^{-1}, $E/D = 0.055$, $g_x = 2.12$, $g_y = 2.13$, $g_z = 2.10$. The first set is associated to the Ni complexes that have the longer Ni–N_{NCS} bond lengths (see ESI,‡ Fig. S4 and S5). These values show that the rhombicity is very weak and D is positive which is expected for a Ni(II) ion having a tetragonal elongation.[13] The weak rhombicity is due to the very small difference in the electronic structure (and bond lengths) between the nitrogen atoms of cyclam that lie in the perpendicular plane. While the relatively large axiality is due to the important electronic difference between the nitrogen cyclam atoms and those belonging to NCS^- since at a basic level NCS^- may be considered as a σ and π-donor ligand while the amines are only σ-donor ligands. Furthermore, the Ni–N_{NCS} bond lengths are longer than the Ni–N_{cyclam} ones. Because of the very close local structure of the Ni(cyclam)(NC)$_2$ unit and Ni(cyclam)(NCS)$_2$, the anisotropy parameters of the latter can be taken as those of the single ion Ni(II) in the trinuclear complex. And the principle axis is reasonably assumed to be along the axial Ni–NC bonds. AOM calculations lead to D and E value for Ni(cyclam)(NCS)$_2$ in good agreement with the experimental data, the anisotropy axis is found as expected along the Ni–N_{NCS} bonds (Fig. 14).[14,15]§ The second mononuclear complex to be considered is (iPrtacn)Cr(CN)$_3$. The analysis of its X-band EPR spectrum leads to the following values for the anisotropy parameters: $D = 0.45$ cm^{-1}, $E = 0$ (ESI,§ Fig. S6). Since the complex has a pseudo three-fold symmetry axis, the z axis is along this symmetry axis. The anisotropy axes of the local tensors of Cr and Ni are shown in Fig. 14, each in its local basis. One can see that because of the bent Ni–N_{CN}–C angle (155.8°), the local z axis on Cr and Ni are almost parallel.

§ The calculation of the spin Hamiltonian parameters D and E that express the magnetic anisotropy of a spin state were carried out using the AOM software where the angular overlap model parameters e_σ and e_π of the ligands surrounding the metal ion and the structure are used as an imput. One of the important point is to be able to choose reliable AOM parameters for a given complex. The parameters used in the present case were taken from related compounds in the literature.[15] It was checked for each case that a slight change of the AOM parameters do not dramatically change the spin-Hamiltonian values obtained. One output of the software is the orientation of the anisotropy tensor $\boldsymbol{D}$ as regards to a local basis that can be chosen at beginning of the computation.

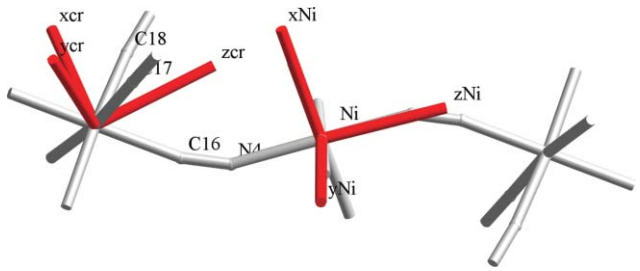

Fig. 14 Orientation of the local Ni and Cr $\boldsymbol{D}$ tensors as regards to the M–ligand bonds for complex **1**.

The application of eqn (1) to the particular case of complex **1** leads to the following tensorial relation:

$$\boldsymbol{D}_4 = 2d_{\mathrm{Cr}}{}^4\boldsymbol{D}_{\mathrm{Cr}} + d_{\mathrm{Ni}}{}^4\boldsymbol{D}_{\mathrm{Ni}} + 2d_{\mathrm{CrNi}}{}^4\boldsymbol{D}_{\mathrm{CrNi}} \quad (2)$$

where $\boldsymbol{D}_{\mathrm{Cr}}$, $\boldsymbol{D}_{\mathrm{Ni}}$ and $\boldsymbol{D}_{\mathrm{CrNi}}$ are the tensors corresponding to the single ion Cr, to the single ion Ni and to the anisotropic exchange interaction, respectively.¶ For metal-oxo complexes with short M–M distances (less than 2.5 Å) and exchange interactions larger than 100 cm^{-1}, the anisotropy coming from the dipolar interactions and from exchange may contribute in a decisive manner to the overall anisotropy.[16] For cyanide bridged complexes, the metal–metal distances are around 5 Å and the exchange interaction parameter is rarely larger than 25 cm^{-1}, one can safely assume that mainly the single ion anisotropy contributes to the overall anisotropy. The application of eqn (2) leads to the following values for the anisotropy parameters of the $S = 4$ ground state: $D_4 = 0.30$ cm^{-1} and $E_4/D_4 = 0.05$.* The calculated values are very close to what was found from EPR (0.312 cm^{-1} and 0.01 for D_4 and E_4/D_4, respectively). This result validates the idea that a good knowledge of the magnetic anisotropy of the model mononuclear complexes allows to compute the anisotropy parameters of the cluster in excellent agreement with the experimental data. The calculations gives the orientation of the anisotropy tensor of the $S = 4$ ground state (Fig. 15). The z axis of the $\boldsymbol{D}_4$ tensor is found as expected in the same direction as the local Cr and Ni tensors. Complex **1** is an interesting example for the validity of our approach that aims to check whether one can predict the nature of the magnetic anisotropy of a polynuclear cluster by using the local anisotropy of model complexes. In the following, we will use the same approach on a more complicated molecule where, as we will see, the principal local anisotropy axes are not collinear.

For complex **2**, the $Ni(Me_2bpy)_2(NC–)_2$ unit was modeled by the mononuclear complex $Ni(bpy)_2(NCS)_2$. The analysis of the EPR

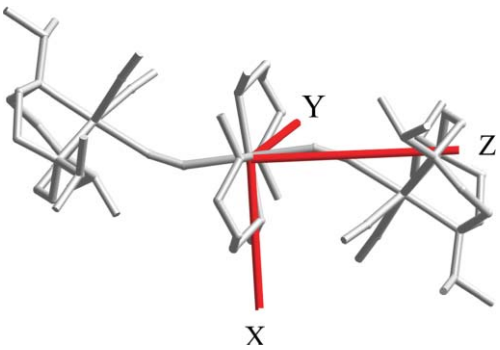

Fig. 15 Orientation of the $S = 4$ $\boldsymbol{D}$ tensor in complex **1**.

spectra of the mononuclear complex recorded at 190 and 285 GHz leads to the following parameters: $D = -1.74$ cm^{-1}, $E/D = 0.24$, $g_x = 2.14$, $g_y = 2.19$ and $g_z = 2.105$ (see ESI,‡ Fig. S7 and S8). The value of E/D close to 0.33 indicates that the rhombicity is strong in this compound compared to that of $Ni(cyclam)(NCS)_2$. Using the AOM software in a similar way as for $Ni(cyclam)(NCS)_2$, it was possible to reproduce fairly well the experimental data (see ESI,‡ Table S5). The calculated values were found to be: $D = -1.65$ cm^{-1} and $E/D = 0.26$ and the orientation of the Ni $\boldsymbol{D}$ tensor axes was determined. Since the orientations of the Ni and Cr local $\boldsymbol{D}$ tensors are known (Fig. 16), it is possible now following the same procedure as above to calculate the $\boldsymbol{D}_5$ tensor elements using the following relation:††

$$\boldsymbol{D}_5 = 2d_{\mathrm{Cr}}{}^5\boldsymbol{D}_{\mathrm{Cr}} + 2d_{\mathrm{Ni}}{}^5\boldsymbol{D}_{\mathrm{Ni}} + 4d_{\mathrm{CrNi}}{}^5\boldsymbol{D}_{\mathrm{CrNi}} \quad (3)$$

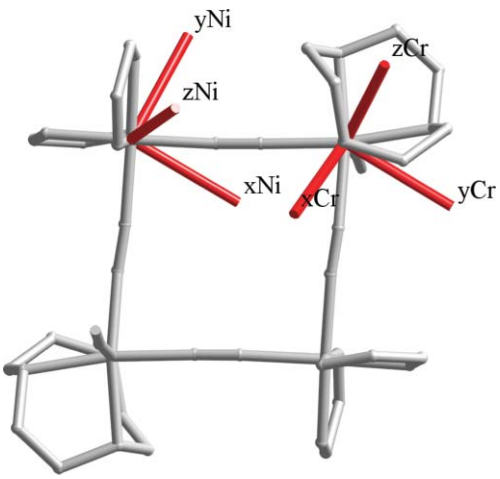

Fig. 16 Orientation of the local Ni and Cr $\boldsymbol{D}$ tensors as regards to the M–ligand bonds for complex **2**.

The principal values of $\boldsymbol{D}_5$ lead to the anisotropy parameters for the ground $S = 5$ spin state: $D_5 = 0.12$ cm^{-1} and $E_5/D_5 = 0.3$. The agreement between the calculated and the experimental values (0.154–0.13 cm^{-1} and 0.31 for D_5 and E_5/D_5, respectively) is reasonably good since the geometry of the parameters of the Ni ion within the complex has some differences with that of the model we assumed. The orientation of the $S = 5$ anisotropy tensor is depicted in Fig. 17.

¶ The $d_i{}^S$ coefficients were calculated by Sessoli using the Genio software. The following values were obtained: $d_{\mathrm{Ni}}{}^4 = 0.0357$, $d_{\mathrm{Cr}}{}^4 = 0.1071$, $d_{\mathrm{NiCr}} = 0.1071$.

* The computation of the D and E values of a given spin state are done as follows: (i) the local $\boldsymbol{D}$ matrices of each metal ion are expressed each in its local basis which leads to diagonal matrices, (ii) all the matrices are then expressed in one common basis using the standard basis change procedure, (iii) one all the $\boldsymbol{D}$ tensors are expressed in one common basis, the sum of the matrices can be done taking into account the $d_i{}^S$ coefficients, (iv) the resulting matrix is diagonalized which leads to the eigenvalues and eigenvectors. This last step leads to a diagonal matrix where the diagonal elements (eigenvalues) have their usual meaning for the $\boldsymbol{D}$ tensor *i.e.* $|D_{11} - D_{22}| = 2E$ and $D_{33} = 2D/3$ which leads the values of E and D of the ground state at hand. The eigenvectors allow to know the orientation of the $\boldsymbol{D}$ tensor of a given spin state with regards to the local basis.

†† $d_{\mathrm{Ni}}{}^5 = 0.022222$, $d_{\mathrm{Cr}}{}^5 = 0.066667$, $d_{\mathrm{CrNi}}{}^5 = 0.066667$.

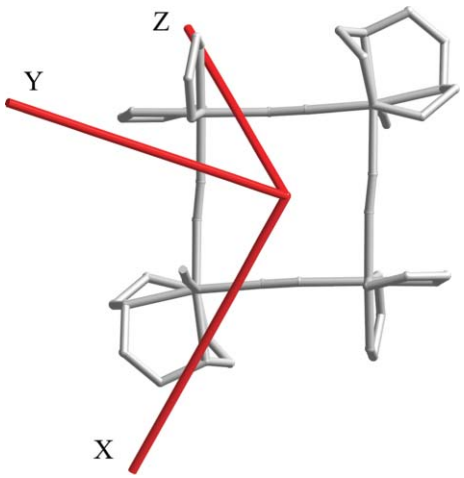

Fig. 17 Orientation of the $S = 5$ $\boldsymbol{D}$ tensor in complex **2**.

In all the calculations performed above the dipolar interactions were neglected. However, we computed this dipolar interaction for **1** and **2** (not reported here) and found values of the order of 0.001 cm^{-1} which justifies the approximation we made.

An ultimate study that has not been carried out yet is the experimental determination of tensors orientation that allows to completely validate our method. This can be obtained by performing EPR studies on single crystals.

Concluding remarks

Three important points merit some comments. The first one concerns the synthesis. The use of the Ni(II) assembling complexes that have available coordination sites in *trans* and *cis* positions for $Ni(cyclam)^{2+}$ and $Ni(Me_2bpy)_2^{2+}$, respectively insures the position of the chromium complexes but cannot give a prediction on the architecture of the final compounds. Even though the reactions are performed under thermodynamic conditions, it is difficult to predict whether the enthalpic or the entropic part will dominates for the stabilization of the final complex. If enthalpy dominates (all the cyanides are bridging), the reaction between $Ni(cyclam)^{2+}$ and $Cr(iPrtacn)(CN)_3$ should lead to a cubic complex with the chromium atoms occupying the vertices and the nickel atoms the centre of the edges. Unfortunately, the trinuclear complex is the output of the reaction with the maximum entropy that seems to be dominating here. Thus, the approach we use is not as rational from the synthetic point of view since many possibilities (but not infinite) for the architecture of the final compounds are obviously possible. The only rational part in this approach is the nature of the exchange coupling interaction (ferro- or antiferromagnetic) that can be predicted in most cases.

The second point concerns the reliability of the computed anisotropy parameters of the clusters. The results obtained show that the calculated values are very close to the experimental ones. Particularly, the sign of D is the right one and even the rhombicity of the ground state found from calculation is mainly the same as the experimental results. This is very encouraging and allows to draw the conclusion, for at least small clusters, that when the building blocks can be reasonably modelled one can have a reasonable idea of the magnitude and the type of anisotropy of a given spin state of the cluster.

The third point concerns the relation between the anisotropy of the assembling complexes and that of the final complex. We will focus on the trinuclear complex **1** where the analysis is simple to make, even though the same conclusions apply on complex **2**. The D value for complex **1** was found equal to 0.312 cm^{-1} much weaker than that of the $Ni(cyclam)(NC–)_2$ unit (5.8 cm^{-1}), even though the orientation of the anisotropy axes of Ni and Cr were almost parallel. The reason to such weak overall anisotropy is that the ground state is a ferromagnetic state *i.e.* arising from the ferromagnetic interaction between the metal ions within the cluster. For the ferromagnetic state, the d_i^S coefficients are found to be very small so that less than 3% of the single ion anisotropy of Ni contributes to the anisotropy of the ground state. This can be understood since the largest anisotropy for an assembly of interacting spins arises for the antiferromagnetic exchange coupling situation (if the resulting spin is not zero) while the weakest anisotropy is found where the spins are parallel. Thus, in order to obtain the maximum anisotropy for a cluster the ground state must result from the antiferromagnetic interaction between the local moments. The drawback is a decrease of the value of S that may well not be compensated by a strong anisotropy leading to an even weaker anisotropy barrier for SMMs.

Acknowledgements

We thank the CNRS (Centre National de la Recherche Scientifique), and the European community for financial support (Contract MRTN-CT-2003-504880/RTN Network "QuEMolNa" and contract NMP3-CT-2005-515767 NoE "MAGMANET"). The authors thank A. Bencini for providing the AOM software, L. Sorace and G. Blondin for fruitful discussions and R. Sessoli for providing the spin angular momentum coupling coefficients.

References

1 (*a*) A. Caneschi, D. Gatteschi, R. Sessoli, A. L. Barra, L. C. Brunel and M. Guillot, *J. Am. Chem. Soc.*, 1991, **113**, 5873; (*b*) R. Sessoli, H.-L. Tsai, A. R. Schake, S. Wang, J. B. Vincent, K. Folting, D. Gatteschi, G. Christou and D. N. Hendrickson, *J. Am. Chem. Soc.*, 1993, **115**, 1804; R. Sessoli, D. Gatteschi, A. Caneschi and M. A. Novak, *Nature*, 1993, **365**, 141; D. Gatteschi and R. Sessoli, *Angew. Chem., Int. Ed.*, 2003, **42**, 268.

2 S. Parsons and R. E. P. Winpenny, *Acc. Chem. Res.*, 1997, **30**, 89; R. E. P. Winpenny, *J. Chem. Soc., Dalton Trans.*, 2002, 1; R. E. P. Winpenny, *Adv. Inorg. Chem.*, 2001, **52**, 1; Z. J. Zhong, H. Seino, Y. Mizobe, M. Hidai, A. Fujishima, S. Ohkoshi and K. Hashimoto, *J. Am. Chem. Soc.*, 2000, **122**, 2952; S. Maheswaran, G. Chastanet, S. J. Teat, T. Mallah, R. Sessoli, W. Wernsdorfer and R. E. P. Winpenny, *Angew. Chem., Int. Ed.*, 2005, **44**, 5044; M. Murugesu, M. Habrych, W. Wernsdorfer, K. A. Abboud and G. Christou, *J. Am. Chem. Soc.*, 2004, **126**, 4766; A. J. Tasiopoulos, A. Vinslava, W. Wernsdorfer, K. A. Abboud and G. Christou, *Angew. Chem., Int. Ed.*, 2004, **116**, 2169; D. M. Low, L. F. Jones, A. Bell, E. K. Brechin, T. Mallah, E. Riviere, S. J. Teat and E. J. L. McInnes, *Angew. Chem., Int. Ed.*, 2003, **42**, 3781.

3 N. Soler, W. Wernsdorfer, Z. M. Sun, D. Ruiz, J. C. Huffman, D. N. Hendrickson and G. Christou, *Polyhedron*, 2003, **22**, 1783; C. Boskovic, M. Pink, J. C. Huffman, D. N. Hendrickson and G. Christou, *J. Am. Chem. Soc.*, 2001, **123**, 9914; Z. M. Sun, D. Ruiz, N. R. Dilley, M. Soler, J. Ribas, K. Folting, M. B. Maple, G. Christou and D. N. Hendrickson, *Chem. Commun.*, 1999, 1973.

4 Long and coworkers reported a similar complex of formula $[\{(cyclam)NiNC\}_2\{Cr(CN)(Me_3tacn)\}](ClO_{42}\cdot 2H_2O$ where the iPr groups on the tacn ligand were replaced by methyl groups and the anion is ClO_4^- instead of NO_3^-: P. A. Berseth, J. J. Sokol, M. P. Shores, J. L. Heinrich and J. R. Long, *J. Am. Chem. Soc.*, 2000, **122**, 9655.

5 J.-N. Rebilly, L. Catala, E. Rivière, R. Guillot, W. Wernsdorfer and T. Mallah, *Inorg. Chem.*, 2005, **44**, 8194.
6 A.-L. Barra, L.-C. Brunel and J. B. Robert, *Chem. Phys. Lett.*, 1990, **165**, 107.
7 J. Glerup and H. Weihe, *Acta Chem. Scand.*, 1991, **45**, 444.
8 T. Ito and M. Kato, *Bull. Chem. Soc. Jpn.*, 1984, **57**, 2641.
9 T. Mallah, C. Auberger, M. Verdaguer and P. Veillet, *J. Chem. Soc., Chem. Commun.*, 1995, 61.
10 L. Toma, L. M. Toma, R. Lescouëzec, D. Armentano, G. De Munno, M. Andruh, J. Cano, F. Lloret and M. Julve, *Dalton Trans.*, 2005, 1357.
11 O. Kahn, *Molecular Magnetism*, VCH, Weinheim, 1993, p. 26.
12 G. Rogez, J. N. Rebilly, A. L. Barra, L. Sorace, G. Blondin, N. Kirchner, M. Duran, J. van Slageren, S. Parsons, L. Ricard, A. Marvilliers and T. Mallah, *Angew. Chem., Int. Ed.*, 2005, **44**, 1876.
13 F. E. Mabbs and D. Collison, *Electron Paramagnetic Resonance of d Transition Metal Compounds*, Elsevier, Amsterdam, 1992.
14 A. Bencini, I. Ciofini and M. G. Uytterhoeven, *Inorg. Chim. Acta*, 1998, **274**, 90.
15 (*a*) A. B. P. Lever, *Inorganic Electronic Spectroscopy*, Elsevier, Amsterdam, 2nd edn, 1984; (*b*) A. Bencini, C. Benelli and D. Gatteschi, *Coord. Chem. Rev.*, 1984, **60**, 131.
16 A. L. Barra, A. Caneschi, A. Cornia, F. Fabrizi de Biani, D. Gatteschi, C. Sangregorio, R. Sessoli and L. Sorace, *J. Am. Chem. Soc.*, 1999, **121**, 5302; O. Waldmann, R. Koch, S. Schromm, J. Schülein, P. Müller, I. Bernt, R. W. Saalfrank, F. Hampel and E. Balthes, *Inorg. Chem.*, 2001, **40**, 2986; D. Collison, M. Murrie, V. S. Oganesyan, S. Piligkos, N. R. J. Poolton, G. Rajaraman, G. M. Smith, A. J. Thomson, G. A. Timko, W. Wernsdorfer, R. E. P. Winpenny and E. J. L. McInnes, *Inorg. Chem.*, 2003, **42**, 5293.

